Apollo: a large, ultra-fast, event-based direct detection camera

Benjamin Bammes[1]*, Michael Spilman[1], Kalani Moore[1], Robert Bilhorn[1]

[1] Direct Electron LP (San Diego, CA USA) * Corresponding Author (bbammes@directelectron.com)

2023 Gordon Research Conference on Volume Electron Microscopy (vEM)

Apollo's unique design for electron counting

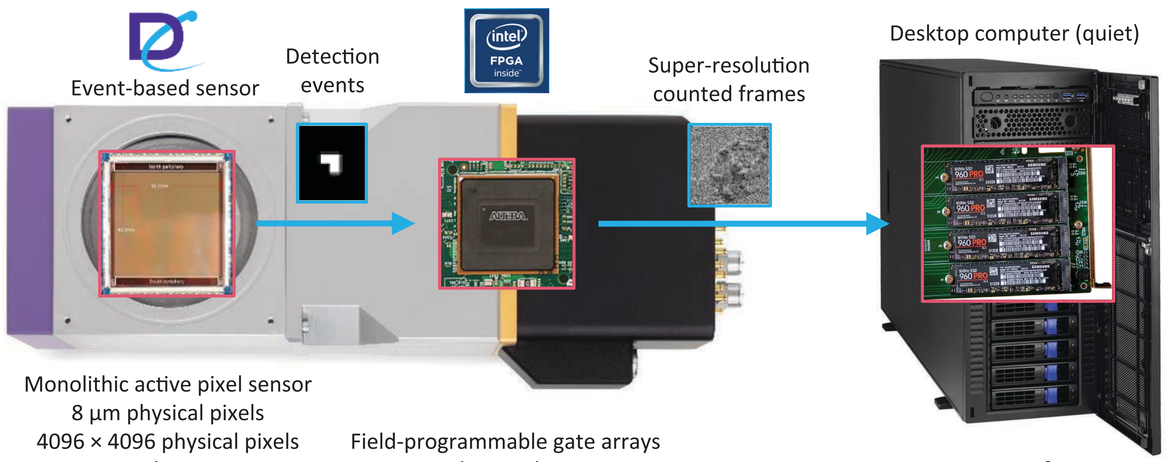

Figure 1: Apollo is based on a novel (US Patent #10,616,521) ultra-fast, event-based, direct detection device (DDD®). The sensor detects incident electrons and outputs the location and shape of each detection "blob" registered on the sensor. Sensor noise is minimized through on-chip correlated double sampling (CDS), on-chip thresholding, and noise-free digital output. The super-resolution centroid of each detected event (which may span multiple pixels) is calculated in FPGA. Detected events are accumulated in 8192 × 8192 dose-fractionated movie frames, which are output to the computer.

Achieving the highest resolution in each lab

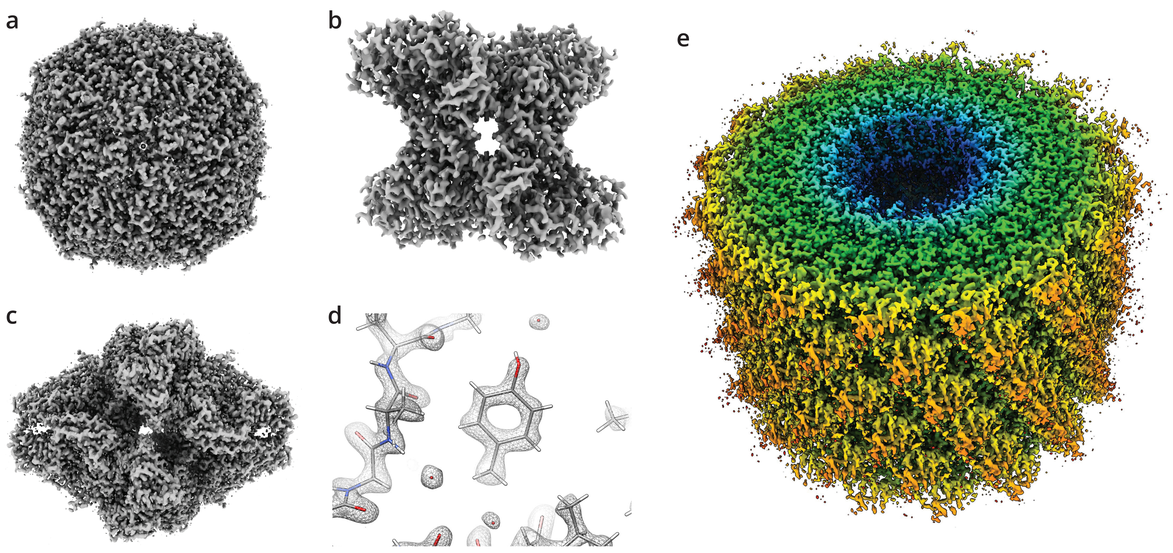

Figure 2: Each cryo-TEM where Apollo is installed has generated its highest resolution reconstructions with Apollo. A few examples are shown here. **(a)** Apoferritin at 1.68 Å from a Titan Krios Gen1 (Florida State University, USA). Data deposited as EMPIAR-11254. **(b)** Aldolase at 2.24 Å from the same lab. **(c)** Beta-galactosidase at 2.0 Å from the same lab. **(d)** Apoferritin at 1.46 Å from a JEOL CRYOARM 300 (JEOL Ltd., Japan). Data deposited as EMPIAR-11101. **(e)** Tobacco mosaic virus (TMV) at 1.85 Å from a JEOL CRYOARM 300 (University of Glasgow, UK). Data deposited as EMPIAR-11404.

MicroED at 0.5 Å resolution

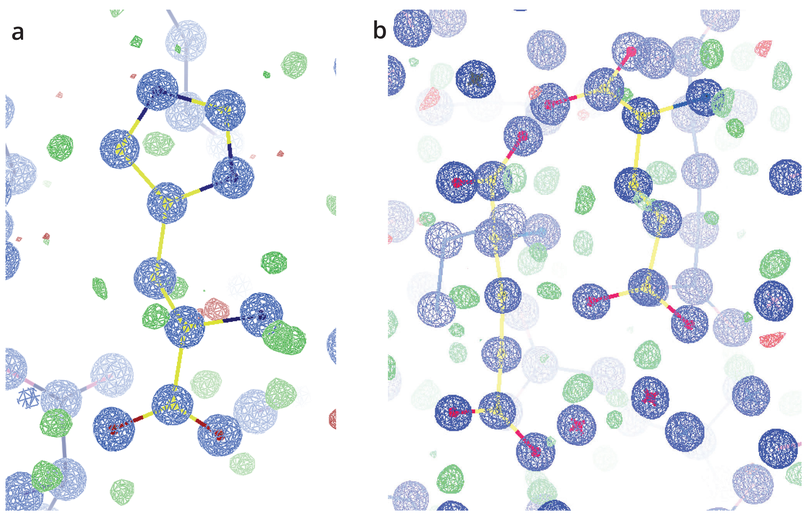

Exposure Rate	0.05 $e^-/Å^2/s$
Tilt Range	-40° to +40°, 2°/s
Acquisitions	12/14 merged

Exposure Rate	0.05 $e^-/Å^2/s$
Tilt Range	-35° to +35°, 1°/s
Acquisitions	14/15 merged

Figure 3: MicroED maps of **(a)** histidine and **(b)** monohydrate sodium glutamate (MSG), both at 0.5 Å resolution, which is the highest known MicroED resolution and only two x-ray crystallography structures in the PDB exceed this resolution (3NIR and 5D8V, both at 0.48 Å resolution). Data was acquired on a JEOL CRYOARM 300 using SerialEM. Low-resolution diffraction spots reached up to ~150 eps. A beamstop was used. Note that the green blobs in the figures are positive differences in density from models without hydrogens. Courtesy of Takanori Nakane (Osaka University).

Minimizing coincidence loss to maximize data quality

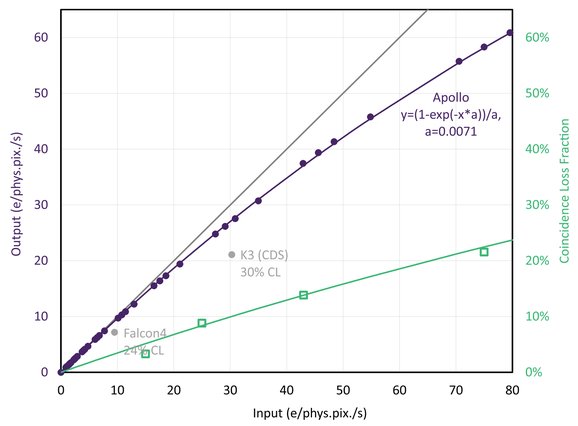

Figure 4: Coincidence loss for Apollo. The dashed line represents the theoretical maximum (absence of coincidence loss). Solid purple circles show the measured output based on the mean intensity of each image compared to the expected input flux. The purple line shows the fit of these data points to the model used in Nakane, et al., 2020. The green line shows the calculated coincidence loss (CL) from the purple line. Outlined green squares show the magnitude of NPS suppression for a few exposure rates. Two solid gray circles show the maximum published exposure response of the Gatan K3 and Thermo Fisher Scientific Falcon4 cameras, as shown in Fig. S1 of Sun, et al., 2023 and Fig. 1e of Nakane, et al., 2020, respectively.

Figure 5: ResLog plots (Stagg, et al., 2014) of apoferritin collected at 3 different exposure rates, showing that higher exposure rate (more coincidence loss) requires more particles to reach any given resolution. To the right are tryptophan densities from each of the highest-resolution maps. Note that Apollo still enabled <1.9Å resolution at nearly 80 eps.

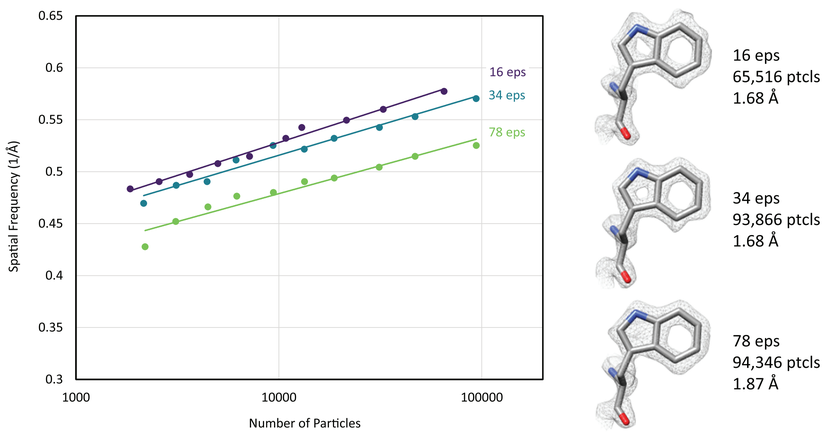

Figure 6: Based on the ResLog plots above, the number of particles necessary to reach any given resolution at 34 or 78 eps (higher coincidence loss) were estimated and then compared to the number of particles needed at 16 eps (lower coincidence loss). Results show that the impact of coincidence loss is magnified at high resolution. The diamonds on each plot show the reconstruction resolution at the best possible "break even point," where the increased throughput due to shorter exposure time compensates for the increased number of particles needed. Note that the true break even point is likely at much lower resolution, because acquisition overhead and computational processing time will reduce throughput considerably.

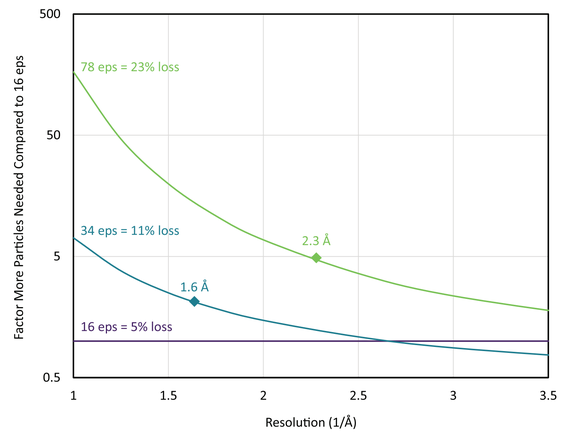

While the speed of Apollo can be used to maximize throughput by acquiring data with a bright beam and a short exposure time, this is likely more useful for screening where the desired resolution is limited. For high-resolution imaging and/or imaging more challenging specimens, the speed of Apollo is better leveraged to maximize data quality by minimizing coincidence loss.

Data in this panel is courtesy of Scott Stagg (Florida State University). For more information, see Peng, et al., 2023, "Characterizing the resolution and throughput of the Apollo direct electron detector," JSB: X 7, 100080.

High-SNR electron tomography

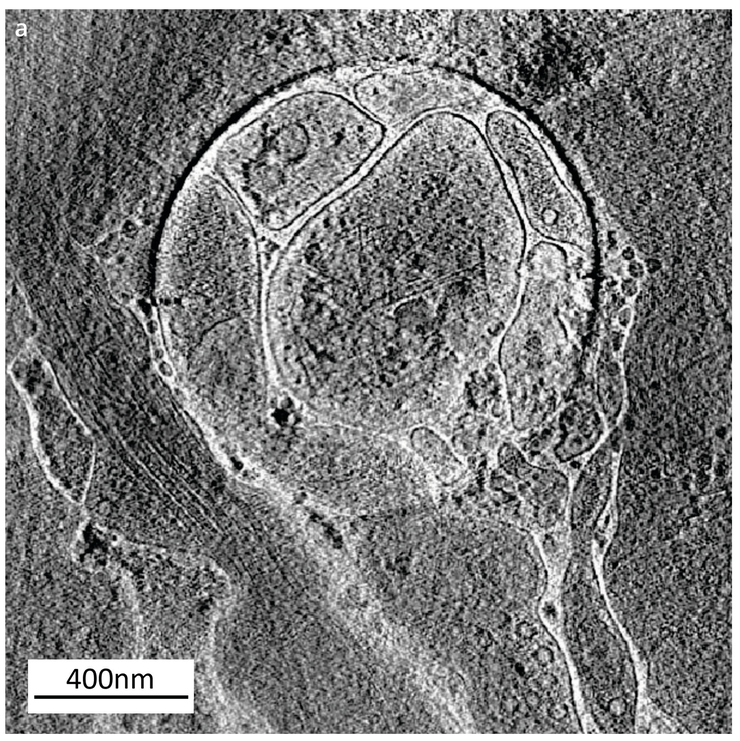

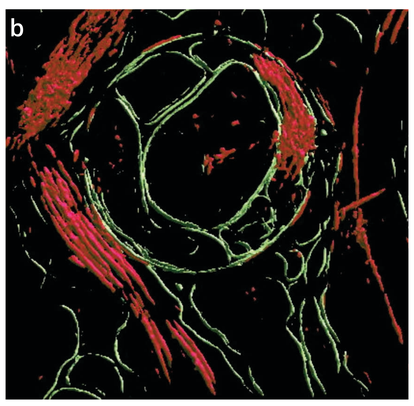

Figure 7: Cryo-tomography of a region of a T-cell, acquired at 200 kV with ~4 µm underfocus and ~85 $e^-/Å^2$ total exposure. Acquisition was dose symmetric from -60° to +60° with 3° tilt step. **(a)** A central slice through the 3D reconstruction. **(b)** Automated segmentation using EMAN2. Courtesy of Erik Anderson & Steve Ludtke (Baylor College of Medicine) and Matt Baker (UTHealth Houston).